

Determining the Condition of Hot Mix Asphalt Specimens in Dry, Water-Saturated, and Frozen Conditions Using GPR

Lanbo Liu^{1,2} and Tieshuan Guo^{1,3}

¹Department of Geology and Geophysics, University of Connecticut, Storrs, CT 06269, USA

²Snow and Ice Branch, Cold Regions Research and Engineering Laboratory, Hanover, NH 03755-1290

³Center for Analysis and Prediction, China Seismological Bureau, Beijing 100036, China

ABSTRACT

A series of laboratory experiments were conducted to measure the dielectric constant of hot mix asphalt (HMA) pavement specimens in dry, water-saturated, and frozen conditions. We used a 1-GHz ground penetrating radar (GPR) system to measure the travel times for direct and reflected waves for computing the electromagnetic (EM) wave velocity. In conjunction with other information on geometry, void ratio, and composition, we computed the dielectric constants of 30 specimens. Our major conclusions are: (1) In general, EM wave velocity is highest in dry conditions, intermediate in frozen, and lowest in water-saturated conditions; (2) EM wave velocity increases slightly with the increase of void ratio for dry samples. In contrast, it decreases significantly with void ratio increase in water-saturated conditions. Correspondingly, the dielectric constant decreases noticeably with an increasing void ratio in dry conditions, and increases appreciably in saturated conditions, in the range of void ratio from zero to 6%; (3) The changes of EM velocity and dielectric constant for dry, saturated, and frozen conditions can be reasonably predicted by the complex refractive index model (CRIM) for porous media; (4) Variations in EM velocity and dielectric constant with respect to asphalt ratio implies that a low asphalt ratio corresponds with a high void ratio; and (5) The observed variations in EM velocity and dielectric constant can be attributed to the change of moisture content of an HMA specimen in different conditions.

Introduction

One of the most important factors affecting the life span and deformation of the hot mix asphalt (HMA) pavements is the void content expressed by the void ratio (Saarenketo, 1997). Void ratio denotes the volumetric fraction of void (or pore) space relative to aggregate solid and asphalt binder of a pavement. The void ratio is important because void space could be filled with air, water, ice, or any fractional combination of these three in a low-temperature environment. Each of these three void materials has different mechanical properties to alter the overall strength of an HMA and influence its durability and stability. For example, the presence of water in void space can significantly change the shear modulus of an HMA pavement. In contrast, the presence of ice in the voids will effectively change an HMA's bulk modulus. Moreover, freeze-thaw processes lower the tensile strength of an HMA pavement and facilitate tensile failure (cracks). Clearly, the amount of moisture penetrating into an HMA pavement, whether from above or below, depends on the HMA's void ratio, and can have detrimental effects on the durability of that pavement. In the last decade, ground-penetrating radar (GPR) has emerged as one of the most widely used non-destructive testing tools in assessing HMA

pavements (Saarenketo, 1992; al-Qadi, 1992; Davis et al., 1994; Maser, 1996; Liu, 1998; Saarenketo and Scullion, 2000).

A rapid and reliable estimation of the void ratio of an HMA pavement is necessary to understand the role of moisture content in HMA durability and stability. Conventionally, HMA void ratio and moisture content have been assessed by direct excavation or drill sampling, or by radioactive methods (Saarenketo, 1997), which are costly and invasive. In this context, if a robust relationship between the electromagnetic (EM) wave velocity, the void ratio and moisture content can be established, non-destructive testing using GPR can be an efficient complementary tool for HMA pavement assessment.

GPR has been used in the field to determine subsurface soil moisture content below highway pavement (Topp et al., 1980; Greaves et al., 1996; Berkold et al., 1998; al Hagey and Muller, 2000; Charlton, 2000; Redman et al., 2002). In laboratory experiments, Saarenketo (1998) reported the effects of water in determining the dielectric permittivity of clay and silty soils. Saarenketo and Scullion (2000) reported the relationship between void content and dielectric constant for dry HMA samples. Shang and Umana (1999) studied the dielectric constant and relaxation time of asphalt pavement materials. In this paper, we report experimental results with

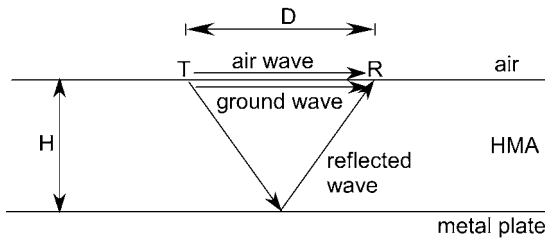


Figure 1. Idealized near surface, near field propagation paths along the interface of the air and an HMA pavement layer with a thickness of H . T: the location of the transmitter; R: the location of the receiver. The separation of T and R is D . The air wave travels from T to R above the surface at the fastest velocity c_0 (speed of light). The ground wave travels from T to R below the surface at a velocity of $c_0/\sqrt{\epsilon_r}$, where ϵ_r is the dielectric constant of the HMA. The reflected wave has a longer ray path: it hits the HMA-base (here a metal-plate) interface, and then is reflected to the receiver.

GPR on HMA specimens in dry, water-saturated, and frozen conditions.

Using a radar system with a 1-GHz antenna, we tested HMA pavement materials in the Connecticut Advanced Pavement Laboratory at the University of Connecticut. The experiments correlated the dielectric constant obtained by GPR measurement with thickness, density, aggregate material composition, and void ratio of HMA specimens under dry, wet, and frozen conditions. Our objectives were to (1) determine the dielectric properties of the asphalt specimens; (2) correlate the dielectric constants with void ratio and asphalt binder content ratio; and (3) elucidate the evolution of the dielectric constant with respect to ambient conditions. These results can be used as a baseline for GPR field surveys over road pavements in real ambient conditions, as well as for quality control for pavement compaction assessment using radioactive methods.

Laboratory Measurements

We tested 30 HMA specimens in dry, water-saturated, and frozen conditions. These cylindrical asphalt specimens were produced at the Connecticut Center for Advanced Pavement Laboratory. They are 15 cm in diameter, about 11.3 cm in height, and are composed of the same aggregate materials. The GPR antenna was set on top of a specimen, which, in turn, was set on a metal (aluminum) plate to gain total reflection (Fig. 1). The use of a metal plate facilitates easy identification of the phase of the reflected waves by providing perfect reflectivity.

The asphalt binder grade (nomenclature for the binder grade is PG 64-28) used for producing these specimens is identical for all samples. The asphalt binder content (AC%)

in any one specimen is given in terms of weight percentage. The samples consist of a range of proportions of aggregates to form a void ratio that varies from 0.5% to 6.0%. The parameters of these 30 specimens are listed in Table 1.

The EM wave velocity of these newly produced HMA specimens were first tested in dry conditions. Each specimen was then submerged in tap water in a sealed container and pumped to extract the air for 10 minutes to reach water saturation. The samples were then submerged in a water tank to hold water-saturated status until testing. These saturated specimens were measured with the 1-GHz GPR again to get the wet velocity. After this, the specimens were immediately refrigerated with a constant temperature of $-18\text{ }^\circ\text{C}$ for 20 hours to reach a frozen state. (Specifications for classic pavement freezing-thawing experiments require the specimen to be frozen no less than 18 hours in one freezing-thawing cycle). Finally, the frozen specimen was tested by the same procedure as was done in dry conditions to get the EM velocity in frozen states. All tests were conducted at room temperature in a time period as short as possible to prevent pore water dripping or thawing. For one specimen in a given condition, at least 10 measurements were taken. The averaged value of the reflected wave travel time from 10 measurements was used to calculate the EM wave velocity in that condition.

Calculations of EM Wave Velocity and Dielectric Constant

We make three justifiable assumptions about the electromagnetic parameters of an HMA to simplify the EM velocity calculation. The first is that velocity does not depend on the magnetic permeability because the asphalt binder and most crushed stones used for making pavement aggregates are essentially non-magnetic. Second, most of the minerals composing the aggregates, such as quartz, mica, and feldspar, are good insulators. The asphalt binder can also be regarded as insulation material. Since the void ratio of an HMA is small, even when the voids are fully saturated with fresh water, the conductivity is still very small. This fact warrants the third assumption that the imaginary part of the dielectric permittivity is negligible. Therefore, EM wave velocity only depends on the real part of the dielectric permittivity.

Velocity Calculation

The electromagnetic (EM) velocity v can be measured in a number of ways. One easy way is to measure the time difference between the direct air wave traveling in air and the ground wave traveling in the HMA (Fig. 1). Unfortunately, for a near-offset (the separation distance between the transmitter and the receiver is very short) survey, the arrival time difference is very small and hard to measure accurately. Another way is the reflection method in which

Table 1. Basic parameters of the HMA specimens used in GPR laboratory experiments.

Specimen Label	Height (cm)	Volume (cm ³)	Dry Weight (g)	Surface wet Weight (g)	Submerged Weight (g)	10-min. vacuum Weight (g)	G _{mm} (g/cm ³)	AC (%)	Void Ratio (%)
A	11.31	1998.647	5062.8	5064.8	3095.8	5070.7	2.589	6.4	0.72
B	11.27	1991.578	5062.2	5066.4	3098.2	5067.2	2.589	6.4	0.57
C	11.25	1988.044	5054.1	5055.5	3092.2	5059.6	2.589	6.4	0.59
D	11.31	1998.647	5066.9	5070.6	3102.3	5082.6	2.626	5.4	2.02
E	11.26	1989.811	5008.9	5015.4	3055.3	5039.8	2.609	5.9	2.05
F	11.33	2002.181	5045.1	5051.7	3086.5	5063.4	2.609	5.9	1.57
G	11.41	2016.318	5053.8	5058.2	3093.1	5065.3	2.609	5.9	1.43
H	11.32	2000.414	5023.7	5029.9	3066.1	5063.3	2.626	5.4	2.63
I	11.36	2007.482	5062.5	5068.2	3086.6	5104.4	2.626	5.4	2.63
J	11.43	2019.852	5046.0	5054.5	3059.0	5116.0	2.626	5.4	3.79
K	11.51	2033.99	5036.8	5046.5	3079.7	5112.8	2.626	5.4	4.06
L	11.38	2011.017	5050.1	5062.7	3079.3	5105.7	2.626	5.4	2.92
M	11.35	2005.715	5058.7	5062.0	3093.6	5077.1	2.609	5.9	1.56
N	11.31	1998.647	5046.7	5050.8	3078.5	5077.1	2.609	5.9	1.85
O	11.36	2007.482	5073.7	5075.3	3097.8	5083.3	2.589	6.4	0.96
P	11.33	2002.181	5082.7	5084.4	3105.2	5089.6	2.589	6.4	0.85
Q	11.35	2005.715	5085.6	5087.0	3104.6	5093.3	2.589	6.4	0.94
R	11.11	1963.304	5010.9	5015.9	3092.0	5035.3	2.665	4.8	2.30
S	11.18	1975.674	5066.6	5055.4	3134.1	5078.7	2.665	4.8	1.87
T	11.07	1956.235	4997.2	5001.9	3085.4	5008.2	2.638	5.3	1.16
U	11.30	1996.88	5023.6	5039.7	3088.0	5068.3	2.661	4.6	2.92
V	11.24	1986.277	5023.4	5039.7	3088.0	5068.3	2.661	4.6	2.35
X	11.48	2028.688	4987.2	5000.2	3060.1	5099.5	2.71	4.0	6.00
Y	11.32	2000.414	5000.2	5005.7	3064.1	5067.7	2.71	4.0	5.50
Z	11.52	2035.757	5019.2	5044.2	3072.2	5109.2	2.71	4.0	5.78
AA	11.30	1996.88	5041.2	5044.3	3052.6	5052.1	2.637	5.5	1.18
AB	11.42	2018.085	5129.8	5135.6	3160.7	5154.0	2.637	5.5	1.54
AC	11.26	1989.811	5029.9	5039.5	3072.8	5061.7	2.637	5.5	1.46
AD	11.20	1979.208	5000.3	5005.6	3079.1	5030.2	2.645	5.1	1.89
AE	11.19	1977.441	5056.7	5061.0	3048.2	5073.4	2.645	5.1	1.35

* G_{mm} is the maximum theoretical specific gravity.

the travel time difference for the direct and reflected waves is the fundamental information for computing EM wave velocity. As shown in Figure 1, the thickness of an HMA is comparable to GPR transmitter-receiver separation. Taking this into account v was calculated by:

$$v = \sqrt{\frac{D^2 + 4H^2}{(t_0 + \Delta t)^2}}, \quad (1)$$

where D is the separation between the transmitter and receiver; H is the thickness of the specimen; t_0 is the direct air wave travel time to the receiver, and Δt is the time difference between the reflected wave from the underlying metal plate and the direct air wave. All parameters on the right-hand side of Eq. (1) are measurable in terms of either geometry or time. For example, the transmitter-receiver

separation is 0.1 m for the 1-GHz antenna of RAMAC/GPR manufactured by MALA Geoscience.

As argued before, due to the justified simplification, the velocity depends only on the real part of the relative dielectric permittivity (the dielectric constant) through

$$v^2 = \frac{c_o^2}{\epsilon_r} \quad \text{or} \quad \epsilon_r = \frac{c_o^2}{v^2}, \quad (2)$$

where ϵ_r is the dielectric constant; and c_o is the electromagnetic wave velocity in vacuum. EM wave velocity and the dielectric constant were calculated by this approach for all of the 30 pavement specimens. A typical time domain radar record is shown in Figure 2. The results of EM velocity and the inferred dielectric constant as functions of the void ratio are shown in Figure 3 and discussed in detail in the next section.

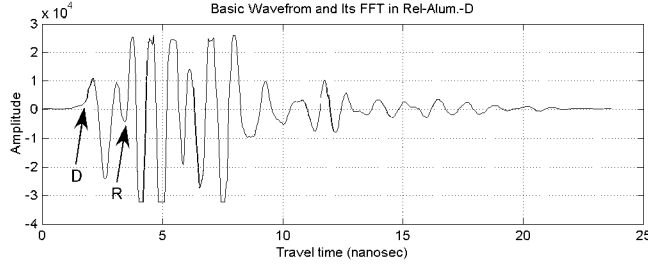


Figure 2. An example of raw waveform of GPR surveys over a dry asphalt specimen which was placed on an aluminum plate. The arrow with letter D indicates the arrival of the direct wave, while the arrow with letter R indicates the arrival of the reflected wave from the aluminum plate.

Results and Discussion

To the first order, the results (Fig. 3) clearly show that the zero-void velocity is about 130 m/ μ s and the zero-void dielectric constant is about 5.3. This implies that the HMA specimens are good dielectric materials and quite transparent in an electromagnetic sense. When the void ratio becomes larger, the EM velocity spreads out among dry, wet, and frozen conditions up to a value of 13% of the reference velocity (130 m/ μ s) when the void ratio is 6%. The corresponding changes in the dielectric constant reach as large as 25%.

The CRIM Model

For analyzing the EM velocity in a porous medium like an HMA, a good approximation for a hybrid material model is a solid skeleton containing void space, with the void filled with two kinds of fluid. A dielectric model formulation commonly used is the complex refraction index

model (CRIM) (e.g., Robert, 1998; al Hagrey and Muller, 2000):

$$n_b = \phi S n_w + (1 - \phi) n_g + \phi(1 - S) n_a, \quad (3)$$

where $n = \sqrt{\epsilon_r}$ is the refractive index, and sub-indices b , w , g , and a represent bulk, water, aggregate, and air, respectively. Also, ϕ is the porosity, and S is the water saturation. The porosity ϕ is related to the void ratio e through

$$\phi = \frac{e}{1 + e}. \quad (4)$$

In the low porosity regime (less than 7%), the porosity and void ratio are not significantly distinguished from each other. We applied the CRIM model to analyze the observed velocity and dielectric constant by using the following parameters. Because the dielectric constant is about 5.5–6.5 for aggregates and 2.6–2.8 for asphalt binder (Saarenketo, 1997), and the asphalt content (AC%) is only about 5% of the total weight of a specimen, the effective dielectric constant of 5.3 was used for the solid matrix (aggregates bonded by asphalt binder). The dielectric constant is 81 for fresh water, 3.17 for fresh water ice (Arcone, 1984), and 1 for air. Replacing n_a by n_i , the refractive index of ice, Eq. (3) was used again to compute the bulk dielectric constant for voids filled with ice-water mix. Using these values, the modeling results for the case of air-water mix filling the void space are shown in Figure 4. The modeling results for the case of ice-water mix filling the voids are shown in Figure 5.

The CRIM model appears to sufficiently interpret the observed results for the dry and wet conditions. When the void ratio increases, the velocity increases slightly for dry conditions and decreases significantly for wet conditions. This is simply due to the fact that a larger fraction of air filling the voids leads to a higher velocity, and a larger fraction of pore water leads to a lower velocity. The curve of $S = 0.8$ may best fit the observed results for wet conditions.

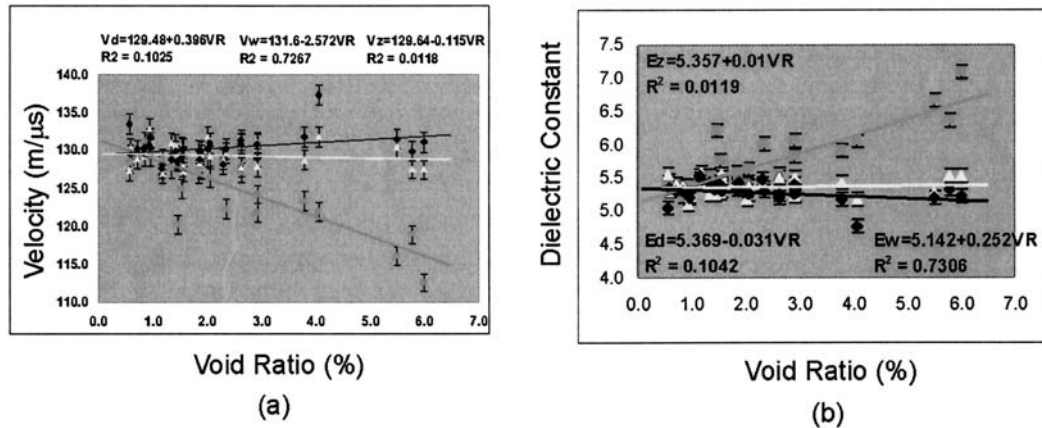


Figure 3. Variations of EM wave velocity (a) and the dielectric constant (b) as a function of the void ratio obtained from GPR measurements of over 30 HMA specimens for dry (Vd and Ed, with blue symbols and lines), wet (Vw and Ew, with magenta symbols and lines), and frozen (Vz and Ez, with yellow symbols and lines) conditions.

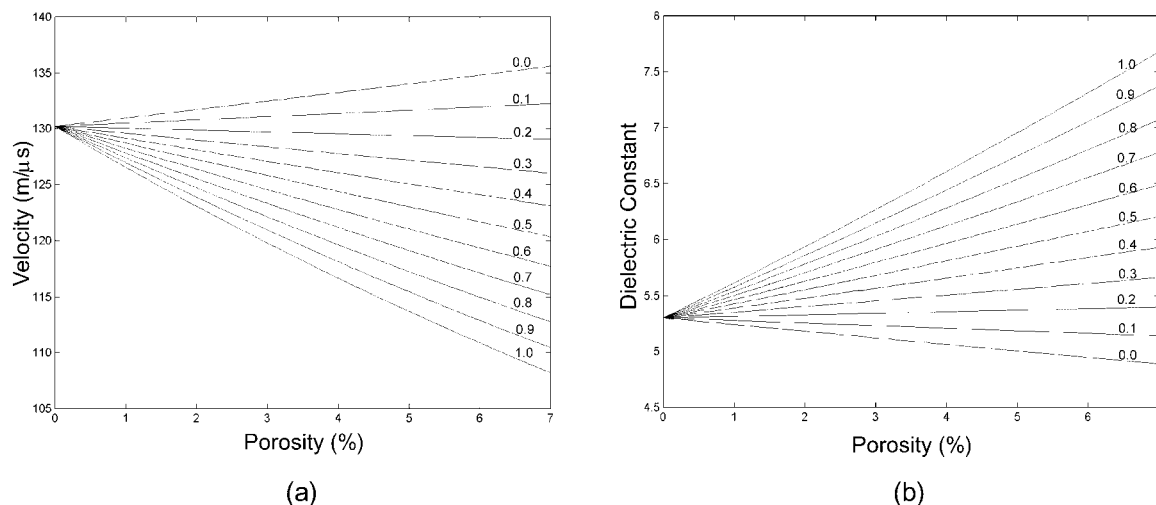


Figure 4. Prediction of EM wave velocity (a) and dielectric constant (b) variations as a function of porosity for water saturation changes from 0 to 1 by the CRIM model. The value of 0.80 best fits the observed results (Fig. 3); it implies that the water-saturation reached about 80% after 10-min air-stripping pumping.

This implies that the pores of the HMA specimens were 80% saturated by water, and 20% filled with air (Fig. 4). This indicates that the 10 minutes of air-stripping pumping in the vacuum process we used to prepare saturated samples was not long enough to reach ideal 100% saturation. In frozen conditions, the CRIM model also predicts that velocity should increase with increase of the void ratio, if there is less than about 15% void space filled with water (Fig. 4a). Actually, the observed trend for the frozen condition (Fig. 3) slightly decreases with increase of the void ratio, and implies that there is about 20% of the pore water remaining unfrozen or being thawed when we took the GPR measurements.

Void Ratio-Asphalt Content Correlation

The relationships between the observed EM velocity and the dielectric constant with respect to the asphalt content were also studied (Fig. 6). The variation trends are opposite to variations of the velocity and dielectric constant with respect to the void ratio (Fig. 3). The EM velocity and the dielectric constant for the dry and frozen conditions do not change at all with variation in asphalt content: the asphalt bitumen is less than 6.5% in an HMA specimen, and so has little effect upon the bulk dielectric constant. An inverse correlation was also found between the void ratio and the asphalt content (Fig. 7). This observed inverse correlation

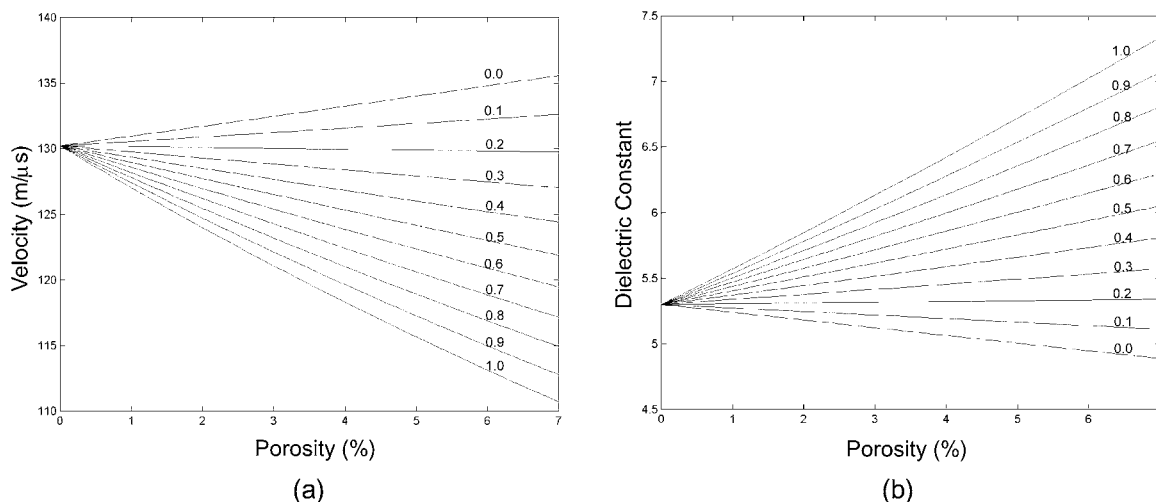


Figure 5. The CRIM predicted EM wave velocity (a) and dielectric constant (b) as a function of porosity for the ice-water mix case. In this case, the void space is filled with only ice and water, no air. Water saturation changes from 0 to 1 correspond to 100% frozen to unfrozen. The curve of water saturation of 0.2 best fits the observed results in frozen conditions (Fig. 3); it implies that 20% of the pore water is still unfrozen after 20-hours freezing in a refrigerator.

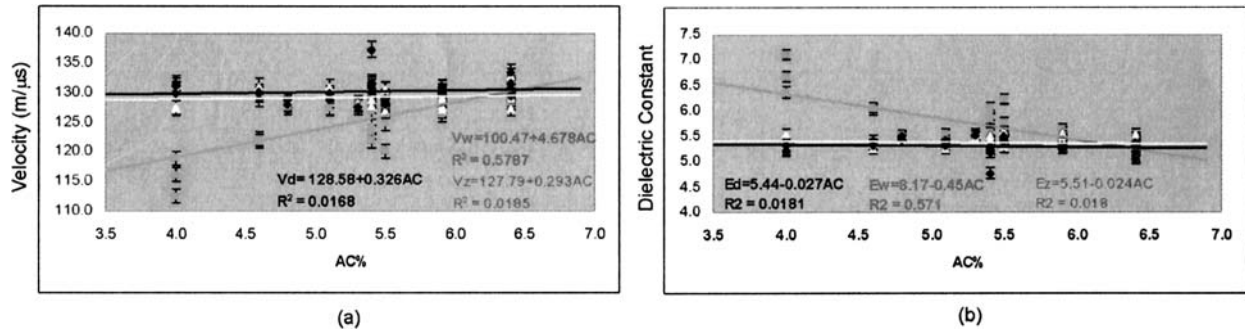


Figure 6. EM wave velocity (a) and dielectric constant (b) variations for 30 HMA specimens as a function of asphalt content (AC%) in dry (Vd and Ed, with blue symbols and lines), wet (Vw and Ew, with magenta symbols and lines), and frozen (Vz and Ez, with yellow symbols and lines) conditions.

implies that lower asphalt content may lead to a larger void ratio. Therefore, the amount of asphalt binder applied to an HMA plays a significant role in optimizing void ratio to construct a durable and stable road surface.

Moisture Content Predicted by the Topp Model

Based on our fitting for the saturated condition, the moisture content varies from zero to 5.6% when the void ratio changes from zero to 7%, with 80% saturation. The EM velocity drops from 130 m/μs to 113 m/μs (Fig. 3a). According to the model (Fig. 8) given by Topp et al. (1980) the moisture content is related to the dielectric constant through

$$\theta_v = -5.3 \times 10^{-2} + 2.92 \times 10^{-2} \varepsilon_r - 5.5 \times 10^{-4} \varepsilon_r^2 + 4.3 \times 10^{-6} \varepsilon_r^3. \quad (5)$$

Using the velocity-dielectric constant relationship given by Eq. (2), for the same range in velocity changes, the predicted

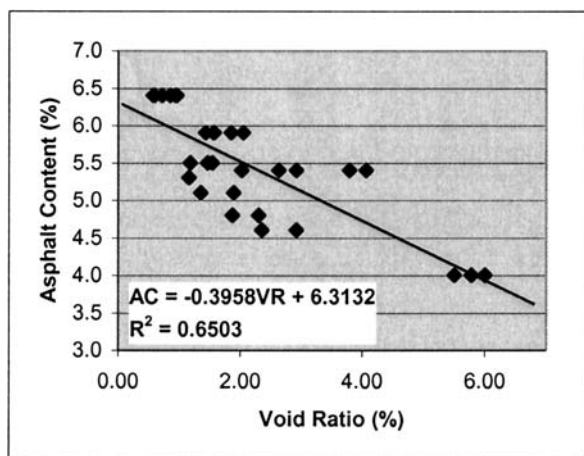


Figure 7. Correlation of void ratio and asphalt content extracted from 30 HMA specimens.

moisture content increase by the Topp model is about 4.2%. Apparently, the observed trend agrees with the Topp model reasonably well; the Topp model slightly under-estimated the moisture changes.

Conclusions

The major conclusions from these experiments are: (1) The EM wave velocity increases slightly with the increase of void ratio for dry HMA specimens. In contrast, it decreases significantly by increasing void ratio in water-saturated conditions. Correspondingly, with the increase of the void ratio, the dielectric constant decreased slightly when the samples were dry, and increased appreciably when the samples were wet. (2) The changes of EM velocity and dielectric constant for dry, wet, and frozen conditions can be sufficiently predicted by the CRIM model for porous media. (3) A comparison of the observed and predicted EM velocity and dielectric constant variations in wet conditions implies that some HMA specimens did not reach full saturation when the GPR measurements were taken. (4) The observed change of EM velocity and dielectric constant in frozen conditions implies that water in the HMA specimens were not completely frozen when the GPR measurements were taken. (5) The variations in EM velocity and dielectric constant with respect to asphalt binder content ratio imply that low asphalt content corresponds to a high void ratio, so that in the lower end of asphalt content EM velocity has the maximum fluctuation among different conditions. (6) The observed variation in EM velocity and dielectric constant was essentially affected by the changes in moisture content, as predicted by the Topp model.

With more GPR and other direct measurements, GPR may prove to be an efficient way to non-destructively detect void ratio, moisture content, and degree of pore water freezing for road pavements. This is of special interest to engineers who are responsible for road inspection and maintenance in cold regions.

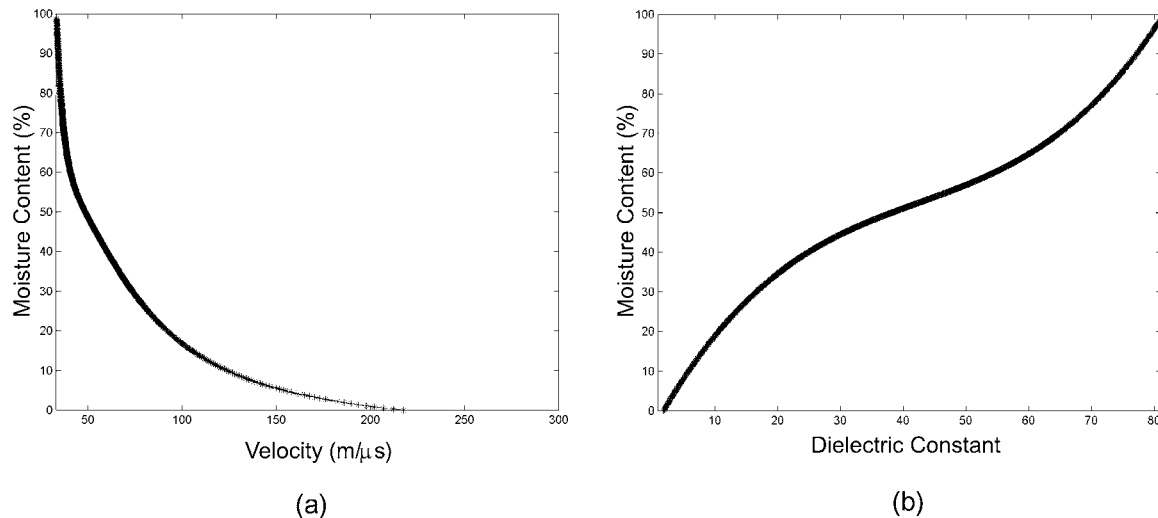


Figure 8. An empirical prediction (Topp et al., 1980) of the moisture content variations as functions of EM wave velocity (a), and the bulk dielectric constant (b).

Acknowledgments

This study was supported by the Connecticut Department of Transportation (ConnDOT) through the Joint Highway Research Advisory Council (JHRAC) Project 00-2. The GPR equipment used in this project was acquired with partial support from the National Science Foundation (NSF-EAR-9712012). One of the authors (TG) is grateful to JHRAC's support for his visiting scholarship while conducting research at the Connecticut Transportation Institute. We are grateful to Drs. Jack Stephens and James Mahoney of the Connecticut Advanced Pavement (CAP) Laboratory for making the CAP laboratory facilities available to this study. Editorial comments from Dr. Steve Arcone of CRREL are highly appreciated.

References

- Arcone, S.A., 1984, Field observations of electromagnetic pulse propagation in dielectric slabs: *Geophysics*, **49**, 1763–1773.
- Berkthold, A., Wollny, K.G., and Alstetter, H., 1998, Subsurface moisture determination with the ground wave of GPR: in Proc. 7th Int. Conf. Ground Penetrating Radar, Lawrence, KS, 675–680.
- Charlton, M., 2000, Small scale soil-moisture variability estimated using ground penetrating radar: in Proc. 8th Int. Conf. Ground Penetrating Radar, Gold Coast, Australia, SPIE Volume 4084, 798–804.
- Davis, J.L., Rossiter, J.R., Mesher, D.E., and Dawley, C.B., 1994, Quantitative assessment of pavement structures using radar: in Proc. 5th Int. Conf. Ground Penetrating Radar, Kitchener, Canada, 319–334.
- Greaves, R.J., Lesmes, D.P., Lee, M.L., and Toksoz, M.N., 1996, Velocity variations and water content estimated from multi-offset ground-penetrating radar: *Geophysics*, **61**, 683–695.
- al Hagrey, S., and Muller, C., 2000, GPR study of pore water content and salinity in sand: *Geophys. Prospect.*, **48**, 63–85.
- Haslund, E., and Nost, B., 1998, Determination of porosity and formation factor of water-saturated porous specimens from dielectric dispersion measurements: *Geophysics*, **63**, 149–153.
- Liu, L., 1998, State-of-the-art rapid non-destructive pavement assessment: Ground penetrating radar (GPR) in monostatic mode: Final Report to the Joint Highway Research Advisory Council, Connecticut Department of Transportation, 57 pp.
- Maser, K.R., 1996, Condition assessment of transportation infrastructure using ground-penetrating radar: *J. Infrastructure Systems*, **2**, 94–101.
- al-Qadi, I.L., 1992, The penetration of electromagnetic waves into hot-mix asphalt: in Proceedings of Nondestructive Evaluation of Civil Structures and Materials, Boulder, CO, 195–209.
- Redman, D., Davis, J.L., Galagedara, L.W., and Parkin, G.W., 2002, Field studies of GPR air launched surface reflectivity measurements of soil water content: in Proc. IX Int. Conf. Ground Penetrating Radar, Santa Barbara, CA, SPIE **4758**, 156–161.
- Robert, A., 1998, Dielectric permittivity of concrete between 50 MHz and 1 GHz and GPR measurements for building materials evaluation: *J. Appl. Geophys.*, **40**, 119–138.
- Saarenketo, T., 1992, Ground-penetrating radar applications in road design and construction in Finnish Lapland: *Geological Survey of Finland, Special Paper* **15**, 161–167.
- Saarenketo, T., 1997, Using ground-penetrating radar and dielectric probe measurements in pavement density quality control: *Transportation Research Record*, **1575**, 34–41.
- Saarenketo, T., 1998, Electrical properties of water in clay and silty soils: *J. Appl. Geophys.*, **40**, 73–88.
- Saarenketo, T., and Scullion, T., 2000, Road evaluation with ground penetrating radar: *J. Appl. Geophys.*, **43**, 119–138.
- Shang, J.Q., and Umana, J.A., 1999, Dielectric constant and relaxation time of asphalt pavement materials: *J. Infrastructure Systems*, **5**, 135–142.
- Topp, G.C., Davis, J.L., and Annan, A.P., 1980, Electromagnetic determination of soil water content: measurements in coaxial transmission lines: *Water Resource Research*, **16**, 574–582.